European Journal of Medicinal Plants

31(3): 56-69, 2020; Article no.EJMP.55481
ISSN: 2231-0894, NLM ID: 101583475

A Study on Heavy Metal Ion Adsorption, Antibacterial and Anticancer Activities of Sawdust Chitosan Activated Carbon

K. Kayalvizhi[1], N. M. I. Alhaji[1*], D. Saravanakkumar[2] and A. Ayeshamariam[3]

[1]Research Department of Chemistry, Khadir Mohideen College (Affiliated to Bharathidasan University, Thiruchirappalli) Adirampattinam, 614701, India.
[2]Department of Physics, Thiagarajar College, Madurai, 625009, India.
[3]Research Department of Physics, Khadir Mohideen College (Affiliated to Bharathidasan University, Thiruchirappalli), Adirampattinam, 614701, India.

Authors' contributions

This work was carried out in collaboration among all authors. Author KK designed the study, performed the statistical analysis, wrote the protocol and wrote the first draft of the manuscript. Authors NMIA and AA managed the analyses of the study. Author DS managed the literature searches. All authors read and approved the final manuscript.

Article Information

DOI: 10.9734/EJMP/2020/v31i330223
Editor(s):
(1) Dr. Paola Angelini, University of Perugia, Italy.
(2) Prof. Marcello Iriti, University of Milan, Italy.
Reviewers:
(1) Kartika Rathore, Jai Narain Vyas University, India.
(2) Abdulsalam Abdullahi, Maryam Abacha American University of Niger, Niger.
(3) Ageng Trisna Surya Pradana Putra, State Islamic University of Sultan Maulana Hasanuddin, Indonesia.
Complete Peer review History: http://www.sdiarticle4.com/review-history/55481

Original Research Article

Received 22 December 2019
Accepted 27 February 2020
Published 28 February 2020

ABSTRACT

Sawdust-Chitosan Composite beads (SDCCB), a low-cost non-conventional surface modified activated carbon, has been used for the efficient removal of Cu(II) ions from aqueous solutions. Surface morphology of the sample has been characterized by XRD, SEM, EDAX and FTIR analyses. Batch experiments have been conducted spectrophotometrically in order to determine the maximum adsorption capacity and influence of physicochemical parameters. The experimental data has been fitted with various isotherm and kinetic models to predict the conditions for maximum adsorption. The activation parameters evaluated for this adsorption process propose the adsorption mechanism as feasible, spontaneous, endothermic and increased randomness. Also, the antimicrobial and anticancer activities of SDCCB have been screened by disk diffusion method and MTT assay, respectively.

**Corresponding author: E-mail: nmialhaji34@gmail.com;*

Keywords: Sawdust; chitosan; adsorption; heavy metal ion; adsorption isotherms; kinetic models; antimicrobial activity.

1. INTRODUCTION

The fast industrialization and the vast use of paints, pigments, fertilizers and electro-engineering techniques cause an abnormal increase in quantity of heavy metals, especially Cu(II) ion, in the environment posing a severe threat to human health. Sawdust can be used to remove these toxic heavy metals from effluents because it has high carbon content, providing beneficial effects on refineries that involve chemical reactions, catalysts, oxidation and reduction materials and so on [1,2]. Conversely, research on sawdust and charcoal utilization in energy science emphasize on the preparation of low cost adsorbents using chemical and electrochemical treatments for the removal of toxic metal ions from aqueous bodies. Cu(II) ions are highly toxic and its excessive presence in water lead to carcinogenetic problems [3,4]. Hence, the present study intends to investigate the preparation of mesoporous untreated and treated sawdust carbon adsorbents in the form of composite beads.

The amino group in chitosan is fully protonated at pH (3-6) and the polymer chains which are positively charged fall apart in solution resulting in dissolution. In order to enhance the resistance of chitosan against acid, alkali and chemicals and to increase its adsorption ability and mechanical strength, cross linking reaction is a crucial step. Different types of cross linking agents such as glutraldehyde, epichlorohydrin, ethylene glycol and diglycinyl ether have been used in cross-linking of chitosan beads [5]. In this study, sawdust-chitosan composite beads (SDCCB) were synthesized using glutraldehyde as cross-linking agent. The results obtained in studies on its surface morphology, adsorption ability, antimicrobial and anticancer activities are presented and analyzed hereunder.

2. MATERIALS AND METHODS

Sawdust was collected from a local saw mill. Analar sample of copper sulphate pentahydrate purchased Aldrich Chemicals was used for the preparation of Cu(II) stock solution. Chitosan, Sodium hydroxide and Glutaraldehyde of analytical grade purchased from Aldrich Chemicals were used as received All other chemicals used in this study were purchased from Merck India. Double distilled water was used for preparing all the solutions. The pH of the study solutions were maintained by hydrochloric acid - potassium chloride mixture for the range of pH 3, acetic acid - sodium acetate mixture for pH 4 – 6 range and boric acid - sodium hydroxide mixture for pH 8 – 10 range. Analytical grade reagent of pottassium ferrocyandie was used to estimate copper ions colorimetrically. Sawdust, collected from a local sawmill was converted into charcoal by 2% of acetic acid and conc. H_2SO_4. The charcoal was converted to sawdust-chitosan composite beads by a procedure reported earlier [6].

The surface area of the prepared SDCCB adsorbent was measured by using BET analyzer (GeminiV2.00 Micromeritics). FTIR measure-ments to identify the functional groups present in the adsorbent were performed in a Perkin Elmer, Dual frontier, equipped with a diffuse reflectance infrared Furrier transformed (DRIFT) collector accessory, using the resolution set at 4 cm^{-1} and 128 scans. The surface morphology was investigated by SEM in a JEOL microscopy, model JSM-7500F. An electron beam with an acceleration voltage of 2 kV was used. The software ImageJ (version 1.45 s) was used for image treatment. The samples were dispersed in isopropanol and deposited in a silicon grid. The morphology was also analyzed by TEM, whose images were obtained in a Phillips microscopy, model CM 200, operating at 200 kV. XRD powder diffractions were acquired using a Simiens D5005 diffractometer with Cu Kα radiation source. The samples were recorded in 5–80º of 2θ, with a step of 0.02º.

Spectrophotometric method was used to estimate Cu(II) ions at 620 nm using Jasco UV-Visible Spectrophotometer to calculate the adsorption capacity (q_e) and percentage removal efficiency by using the equations (1) & (2).

$$q_e = (C_o - C_t)V/m \quad (1)$$

Percentage removal

$$= [(C_o - C_f)/C_o] \times 100 \quad (2)$$

where C_o and C_e are the initial and equilibrium concentrations (*mg*/*l*), *V* is the volume of solution (*l*), q_e is the adsorbed quantity (*mg*/*g*), *m* is the weight of adsorbent (*g*) and C_f is the solution

concentration at the end of the adsorption process (*mg/l*).

Batch adsorption studies were conducted by shaking 25 mL of desired quantity of adsorbate solution with 0.5 gm adsorbent at 200 rpm speed with optimum pH 5 and temperature 303 K. Desorption was carried out by agitating the Cu-adsorbed SDCCB with 25 ml of NaOH solution for 3 hrs. After desorption the sample was washed and neutralized with distilled water [7].

3. RESULTS AND DISCUSSION

3.1 XRD Analysis

Activated carbon has a large chemically active surface area; a characteristic which offers the support of semiconductor nanoparticles. Crystalline phases were evaluated by X-ray diffraction (XRD) technique (Fig. 1). The JCPDS file No-82-0505, is well matched with the reported results of activated carbon [28]. The diffraction plane is (220) with cubic structure. The d_{std}-spacing in the diffraction plane is (5.0416 Å) is nearly equal to d_{obs} (5.123 Å) and the lattice constant is nearly equal to (13.98 Å) which is in well agreement with the reported result of (14.26 Å) [8]. The crystallite size of activated carbon is nearly equal to 51 nm.

3.2 SEM and EDAX Analysis

The surface morphology of SDCCB obtained using scanning electron microscope is shown in Fig. 2a. These image indicate the surface texture and porosity of the adsorbent. Surface coverage in the form of sphere is evident, showing the presence of inorganic elements as confirmed by EDAX analysis as shown in Fig. 2b. Based on the particle morphology, these materials are suitable to be used as adsorbent. The image exhibits abundance of roughness and more crispy nature which may be propitious to its adsorption ability and many pores are clearly found on the surface. Porous structure appears as elongated fibrous particles and well-developed pores lead to the large surface area. The specific surface area of SDCCB as found out by BET analysis is 30 m^2/g [9].

The elemental analysis of SDCCB was done by using EDAX analysis (Fig. 2b). The data are listed in Table 1 establish that the major component present in the sample is carbon, in addition to Ca, Si and Na. On acid treatment these elements are washed or diminished [10].

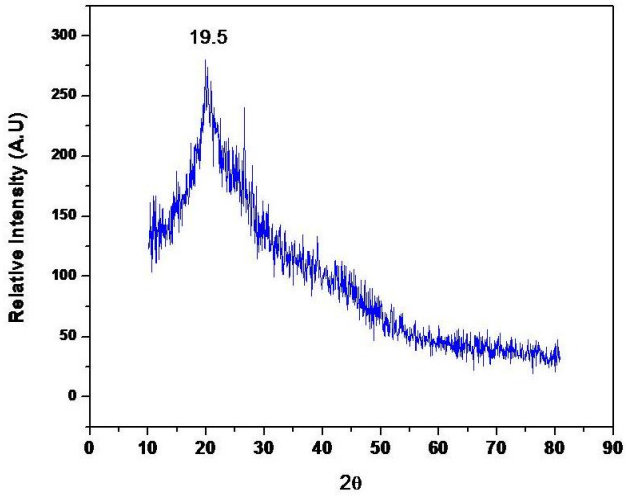

Fig. 1. XRD analysis of SDCCB

Table 1. EDAX analysis of SDCCB

Element	Net counts	Weight %	Atom %
C	7208	70.87	95.52
C	2700	27.00	2.20
Ca	62	2.13	2.28
Total		100.00	100.00

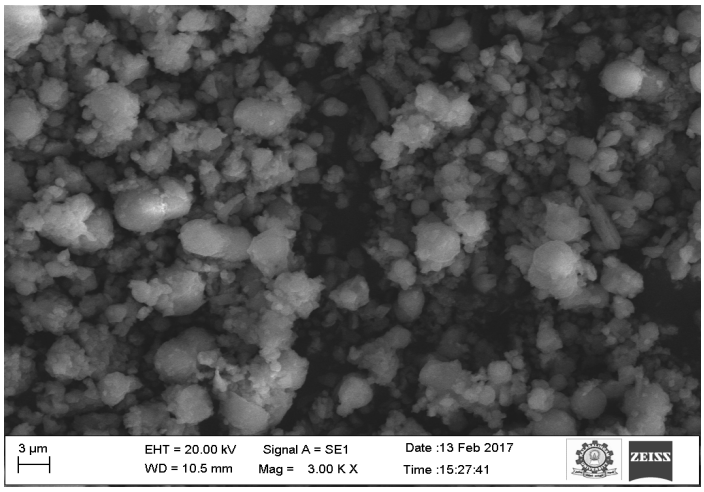

Fig. 2a. SEM image of SDCCB

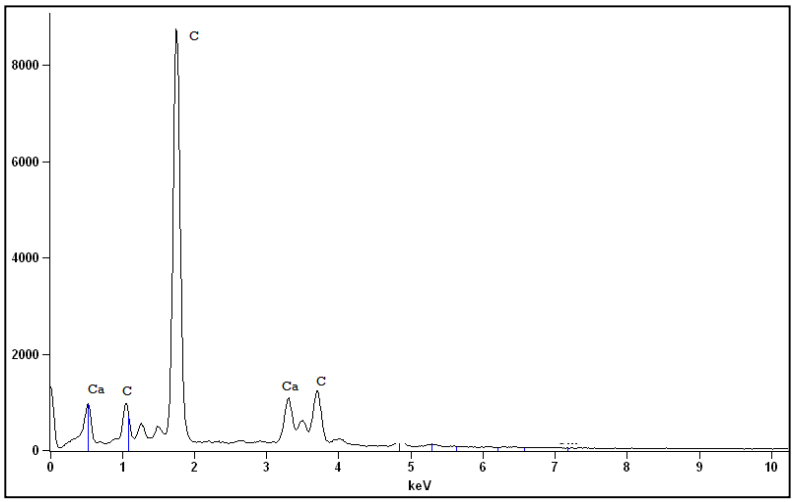

Fig. 2b. EDAX analysis of activated carbon adsorbent

3.3 FTIR Analysis

FTIR spectrum of SDCCB is shown in Fig. 3. Activation of sawdust chitosan activated carbon adsorbent by acid treatment induces many polar functional groups like O-H, C=C, C-N stretch, C-O symmetric stretch, *etc.* and also shifts in transmittance. The Introduction of –N,-O, -S etc. are responsible for stretching and bending vibrations. Wavenumbers of same functional groups are observed for the metal ions as indicated in the spectra of Cu(II) adsorbed sample shown in Fig. 3. The position of peaks indicates that Cu(II) ions are well associated with surface functionality [11] Stretching and bending frequencies are responsible for the incorporation of hetero atom in activated carbon matrix of the adsorbent. So SDCCB is considered an efficient adsorbent for Cu(II) ions because positively charged pollutants may be more easily removed by activated carbons [12].

Effect of pH: Adsorption of metal ion depends on solution pH which influences the electrostatic binding of ions to corresponding functional groups. At different pH values, the Cu(II) adsorption capacity was calculated. It was found that as pH increases from 2 to 5, the adsorption capacity linearly increases and then starts decreasing after pH 5. Thus, maximum adsorption of Cu(II) occurs at pH 5.0 and may be attributed to strong electrostatic binding on the acidic surface of SDCCB as the amine groups in chitosan is protonated to form NH_3^+ groups [13].

Hence, the optimal value of pH for further adsorption studies is considered as 5.0.

Kinetic Models: Adsorption kinetics must be taken into account since they explain how fast the adsorption occurs and also provide information on the factors affecting the adsorption rate. The kinetics of removal of Cu(II) ions from aqueous solutions by SDCCB was studied spectrophotometrically by measuring the absorbance at 620 nm at regular time intervals. Four kinetic models [14], the pseudo first-order, pseudo second-order, intraparticle diffusion and simple Elovich, were tested to investigate the rate of adsorption of Cu(II) ions onto SDCCB using the date listed in Table 2.

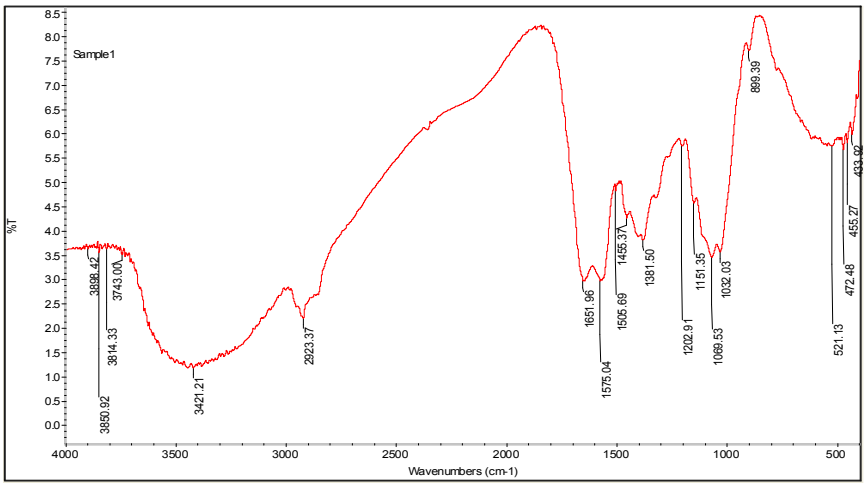

Fig. 3. FTIR analysis of SDCCB

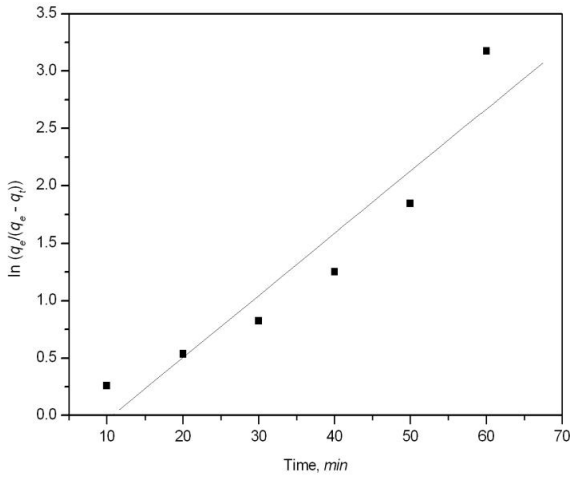

Fig. 4 Pseudo first order kinetic plot for the adsorption of Cu(II) onto SDCCB

Table 2. Data for adsorption kinetic models on adsorption of Cu(II) ions onto SDCCB

Time, min	C_t, mg/l	q_t, mg/g	q_e, mg/g
10	40.1	0.495	2.155
20	32.1	0.895	2.155
30	25.8	1.210	2.155
40	19.2	1.540	2.155
50	13.7	1.815	2.155
60	8.7	2.065	2.155
70	6.9	2.155	2.155

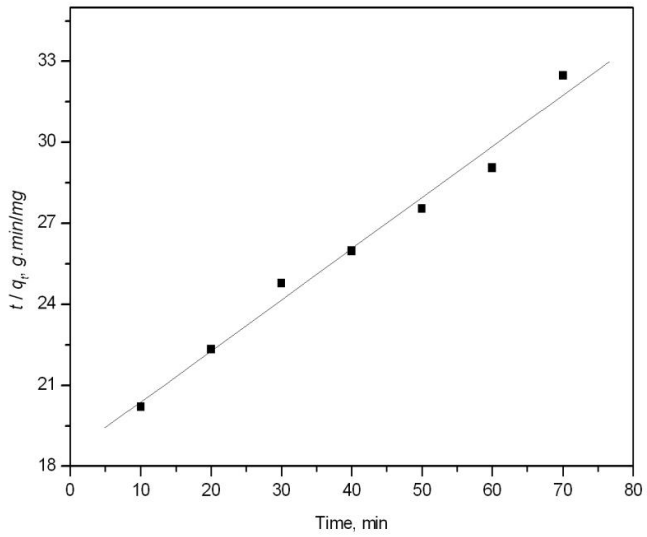

Fig. 5. Pseudo second order kinetic plot for the adsorption of Cu(II) onto SDCCB

The pseudo-first-order and pseudo-second-order kinetic models are useful for determining whether the adsorption is physical or chemical process. If the pseudo-first-order model provides better fit result, then the adsorption is a physical process and if the pseudo-second-order model fits better, then it is a chemical adsorption. Several reactions in general follow chemisorption initially and that too over a very short period of time shown in Figs. 4 and 5.

Elovich kinetic and Inraparticle diffusion kinetic plots were studied to explain the adsorption. If there is equilibrium we get macro-kinetic equation. These adsorption studies with copper(II) heavy metal on activated carbon using adsorbent are shown in Figs. 6 and 7.

The parameters calculated from the slope and intercept values of the linear plots for the four kinetic models collected in Table 3 indicate that adsorption reaction follows pseudo second order kinetics, meaning that rapid adsorption occurs initially due to ion-exchange and followed by slower adsorption because of diffusion of ions into pores for longer duration. Since the line in intraparticle diffusion kinetics does not pass through the origin, it is inferred that chemisorptions is the rate-controlling step, rather than the diffusion process [15].

3.4 Selection by Error Analysis

The linear regression and the non-linear Chi-square analysis gave different models as the best-fitting model for the given data set, thus indicating a significant difference between the analytical methods. Ho [16] reported that the non-linear Chi-square test provided a better determination for the experimental data. In this study, both coefficients of correlation (r^2) and Chi-square (χ^2) test statistics were used for the determination of best-fitting model with the experimental data.

The mathematical equation was given by the equation

$$\chi^2 = \sum \frac{\left(q_e - q_{e,m}\right)^2}{q_{e,m}}$$

where $q_{e,m}$ is the equilibrium capacity obtained by calculation from model (*mg*/*g*) and q_e is the equilibrium capacity (*mg*/*g*) determined from the experimental data. If data from the model are similar to the experimental data then χ^2 would be a small number and vice versa [17]. In linear analyses the different forms of equation would affect the regression coefficient (r) and coefficient of determination (r^2) value significantly and it will affect the final determination. This can be avoided by using nonlinear chi square test analysis. For the first and second order pseudo order models, the correlation coefficients are 0.947 and 0.991 for the adsorption of Cu(II) ions. Correlation between the actual and predicted values of % removal of Cu(II) ions is shown in Fig. 8.

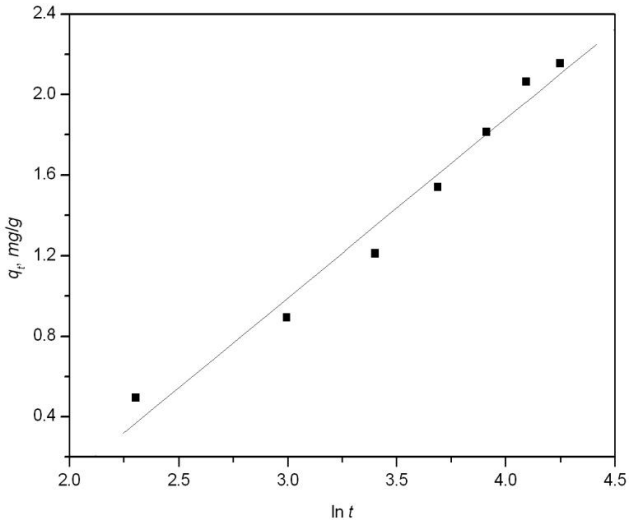

Fig. 6. Simple Elovich kinetic plot for the adsorption of Cu(II) onto SDCCB

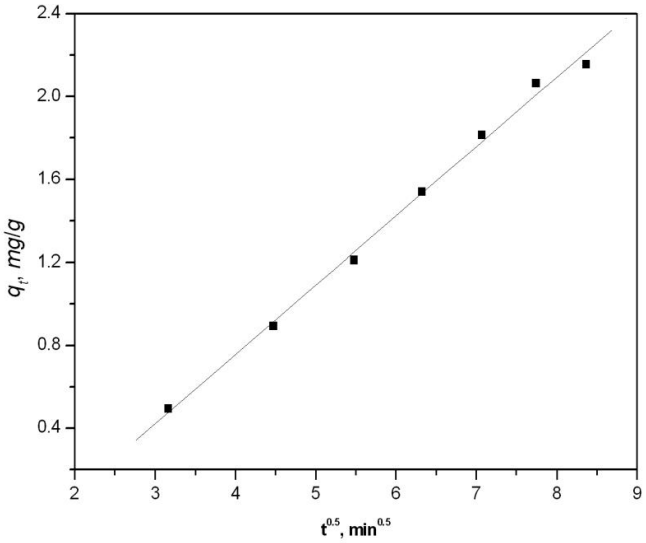

Fig. 7. Inraparticle diffusion kinetic plot for the adsorption of Cu(II) onto SDCCB

Table 3. Summary of parameters derived for various kinetic models

Kinetic model	Equation	Constant	Values for Cu(II)
Pseudo First order	$\ln (q_e - q_t) = \ln q_e - k_1.t$	k_1 (min^{-1})	0.0541
		r	0.947
Pseudo Second order	$t/q_t = 1/k_2.q_e^2 + t/q_e$	k_2 (*g/mg.min*)	0.0019
	$h = k_2 q_e^2$	q_e (*mg/g*)	5.283
		h (*mg/g.min*)	0.0541
		r	0.991
Simple Elovich	$q_t = \beta \ln t + \beta \ln \alpha\beta$	α (*mg/g.min*)	0.1697
		β (*g/mg*)	0.8910
		r	0.987
Intra Particle Diffusion	$q_t = k_{id}.t^{0.5} + C$	k_{id} (*mg/g.min*)	0.334
		C_1, C_2	0.578
		r	0.998

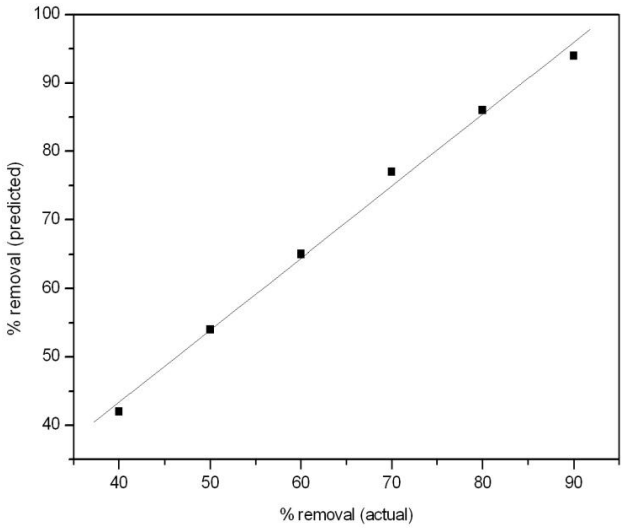

Fig. 8. Correlation between actual and predicted values of percentage removal of Cu(II) ions by SDCCB

3.5 Effect of Temperature

Temperature is an important factor as it reveals additional information about the adsorption process. The Cu(II) adsorption capacity of SDCCB was determined at different temperatures and the result is illustrated in Fig. 9. The increase in adsorption capacity with increase in temperature may be attributed to the formation of some new adsorption sites and enlargement of the pores on the surface of the adsorbent. Also, it implies that adsorption capacity largely depends on the chemical interaction between the functional groups on the adsorbent surface and adsorbate. Thermodynamic parameters were determined from the slope and intercept values of van't Hoff plot (Fig. 10) and the values ΔG^o = -2.932 kJ/mol, ΔH^o = 16.289 kJ/mol, ΔS^o = 60.99 $JK^{-1}mol^{-1}$ and E_a = 18.809 kJ/mol. These thermodynamic parameters can be explained based on the chemical bonding nature of the absorbent-adsorbate interaction [18,19]. The negative ΔG and positive $\Delta H°$ and $\Delta S°$ values indicate that this adsorption is a feasible, spontaneous, endothermic, increased randomness and non-specific chemisorption process.

3.6 Regeneration Studies

Desorption studies were also conducted to explore the feasibility of recycling the adsorbents and recovery of the metal resources. Sodium hydroxide was used for the stripping section for Cu(II) ions [20]. Desorption experiments were conducted by mixing 0.25 g of spent adsorbent with 25 ml of 1 M NaOH. In order to determine the reusability of the adsorbent, the adsorbent was taken out from the solution and washed with double distilled water and protonated with 0.1 M HCl. Consecutive adsorption and desorption studies were repeated six times by using the same adsorbent and is shown in Fig. 11, which indicates stability of the adsorbent [21].

The % removal and hence the adsorption capacity decreases slightly after each cycle and even after the fifth cycle, the sample possesses 82% adsorption capacity. The recovery experiments show that metal ions are retained by the matrix in non-labile forms and that the acid-base reactions are more effective for their displacement than complexation processes.

The recovery experiments show that metal ions are retained by the matrix in non-labile forms and that the acid–base reactions are more effective for their displacement than the complexation processes.

3.7 Bacterial Studies

In a cellular environment, engineered nanomaterials may disturb the oxidative balance of the cell. This phenomenon is called Oxidative stress and it results in Reactive Oxygen Species (ROS) such as superoxide (O_2^-), hydroxyl radical ($HO^·$), peroxy radical ($ROO^·$) and hydrogen peroxide (H_2O_2) or Reactive Nitrogen Species (RNS) such as nitric oxide ($NO^·$), peroxynitrite

anion ($ONOO^-$), peroxynitrous acid (ONOOH) and nitrosoperoxycarbonate anion ($ONOOCO_2^-$).

Antibacterial and antifungal activity of SDCCB was tested using well diffusion method [22]. The prepared culture plates were inoculated with different selected strains of bacteria using streak plate method.

To determine the bacterial resitive efficiency of the sample and evaluate the antibacterial mechanism by generating, releasing, damaging and contact killing sucessively, the stickeed microbials were separated from the surfaces and grown in bacterial culture plate. Wells were made on the agar surface with 5 mm cork borer. The extracts were poured into the well using sterile syringe. The plates were incubated at 37 ± 2°C for 48 hours for fungal activity and for 24 hours for bacterial activity. The plates were observed for the zone formation around the wells. The zone of inhibition was calculated by measuring the diameter of the inhibition zone around the well (in mm) including the well diameter. The readings were taken in three different fixed directions in all 3 replicates and the average values were tabulated. The mechanism is shown in Fig. 12.

In order to make the inhibition, ROS first disturb the capsule, cell wall, cell membrane, cytoplasm and chromosome successively by making the action of depolarization effect among the parts of cell division. This electrostatic stress can be sustained by the electromagnetic interaction experiencing by the samples. In the mechanism, the generated free radicals and e^- can be captured and bounded by the sample adsorbent nanoparticles due to the construction of the Schottky barrier at the interface of chitosan t/C* (activated carbon), overpowering e^-/ h^+ recombination and thus initiate oxidation and reduction quantum yields. The generated h^+ will be reacted with the on-surface of hydroxyl ions or H_2O molecules and generate •OH radicals as well as simultaneously transform into H_2O_2 molecules where the •OH radicals have relatively short lifetime. These produced radicals will make the contact killing mechanism. The observed results reveals the suppression of both staphylococcus aureus and streptococcus pyogenes cells on the surfaces of entitled adsorbent and can be attributed to the damage of the boundary of bacterial membrane and we can see this effect as shown in Fig. 13(a-b), which includes zone of inhibition (ZOI). The Table 4 explains that the zone of inhibition increases with respect to quantity of sample, which is depicted in the bar diagram Fig. 13c. Therefore, the adsorbent has a certain antimicrobial activity on both gram positive bacteria [23].

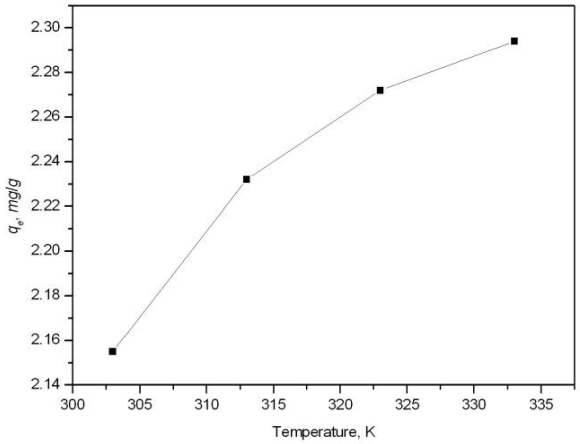

Fig. 9. Effect of temperature on the Cu(II) adsorption capacity of SDCCB

Table 4. Antibacterial activity of SDCCB for 3 different dosages

S. no.	Bacteria	Zone of Inhibition (mm)		
		SDCCB		
		5 mg	10 mg	25 mg
1	Staphylococcus aureus	6	7	12
2	*Streptococcus pyogenes*	11	8	14

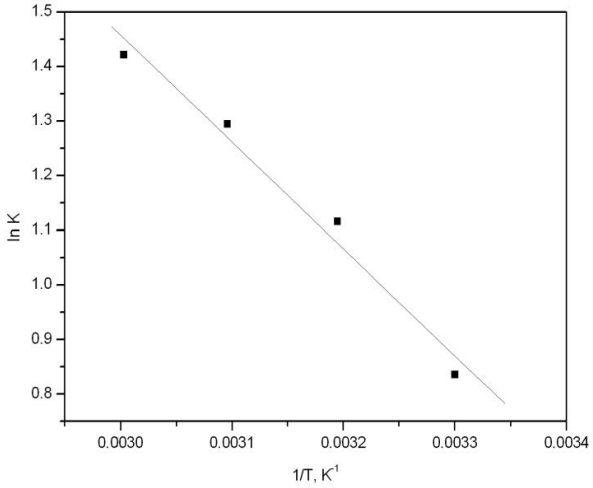

Fig. 10. Van't Hoff plot for the adsorption of Cu(II) ions on SDCCB

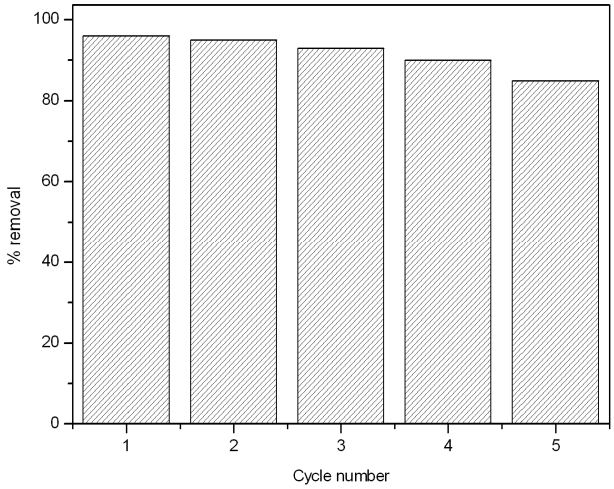

Fig. 11. Reusability of SDCCB for the adsorption of Cu(II) ions

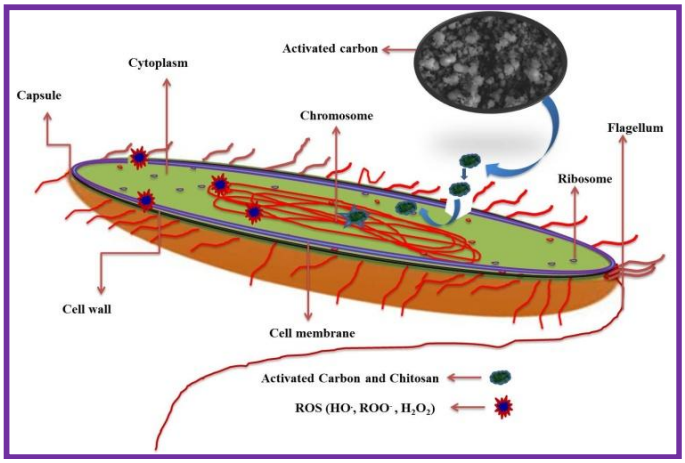

Fig. 12. Antibacterial mechanism shown by SDCCB

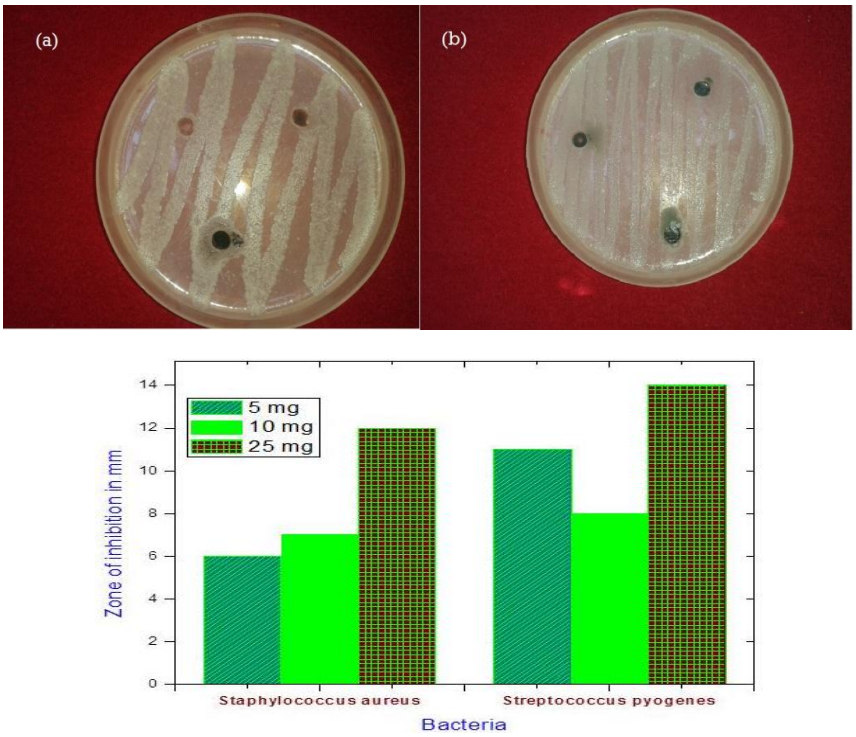

Fig. 13(a-c). Antimicrobial activity of SDCCB

3.8 Images of A549 (Liver Cancer Cell Line)

To study the *in vitro* cytotoxicity of the SDCCB, MTT assay was performed against A549 Liver cells line. The cell viability was calculated after 48 h of incubation of samples treated with cell lines by the formula [24]:

$$\text{Cell viability \%} = \left(\frac{Mean\,OD}{Controlled\,OD}\right)\times 100$$

The cell viability is tabulated in Table 5 and the respective graph is plotted against concentration versus cell viability (%) for both A549 Liver cells lines of sample as shown in Fig. 14 (a-d). The results show that the cell viability decreases with increase in concentration and the IC50 value [25].

The cytotoxicity of SDCCB was evaluated against Liver cell line (A549) via MTT assay [26,27]. The results presented in Table 6 exhibit significant inhibitory activities against Liver cell line (A549) at the three doses of 1000, 31.2 and 7.8 µg/mL. On comparison of the data, it can be inferred that the adsorbent exhibits higher inhibitory activity at the dose of 7.8 µg/mL.

Table 5. Cytotoxicity effect of SDCCB on A549 cell line

S. no.	Concentration (µg/ml)	Dilutions	Absorbance (O.D)	Cell viability (%)
1	1000	Neat	0.042	7.82
2	500	1:1	0.078	16.70
3	250	1:2	0.132	24.09
4	125	1:4	0.175	31.30
5	62.5	1:8	0.213	45.37
6	31.2	1:16	0.245	52.38
7	15.6	1:32	0.309	59.87
8	7.8	1:64	0.312	60.35
9	Cell control	-	0.504	100

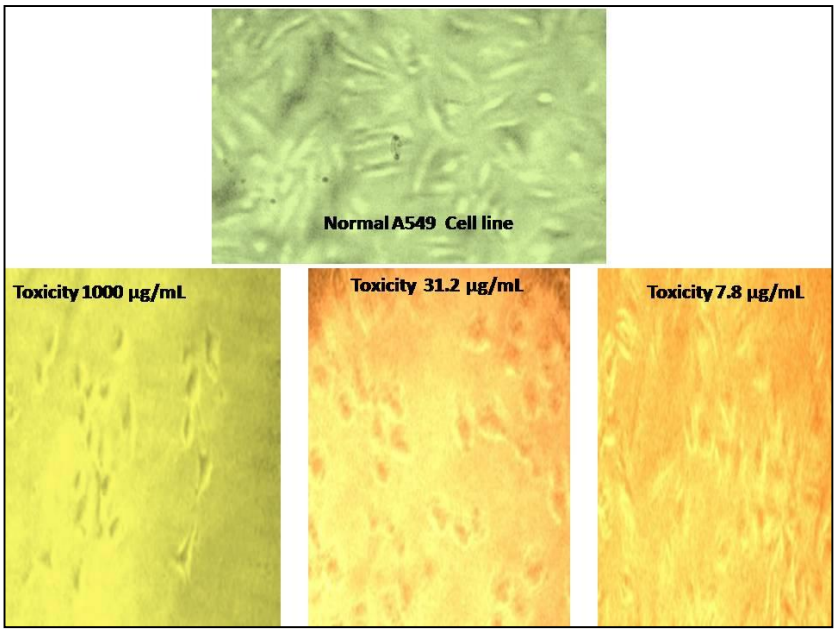

Fig. 14 (a-d). Anticancer effect of SDCCB on A549 cell line

Table 6. Results of the anticancer effect of SDCCB on A549 cell line

S. no.	Concentration (µg/ml)	Dilutions	Absorbance (O.D)	Cell viability (%)
1	1000	Neat	0.036	6.08
2	500	1:1	0.089	16.02
3	250	1:2	0.139	26.04
4	125	1:4	0.171	33.16
5	62.5	1:8	0.213	41.11
6	31.2	1:16	0.266	49.19
7	15.6	1:32	0.301	58.21
8	7.8	1:64	0.326	61.55
9	Cell control	-	0.520	100

4. CONCLUSION

The adsorption of Cu(II) ions occurs through ion-exchange process because of the existence of ionic active species only. Rate of sorption follows the pseudo second order kinetics for Cu(II) ions. These chemisorptions are also confirmed by the validity of intraparticle diffusion model. The thermodynamic study further reveals the endothermic, randomness and feasibly spontaneous nature of the adsorption processes. Regeneration of sawdust-chitosan activated carbon adsorbent is possible and the acid–base reactions are effective upto five cycles. These results suggest that mesoporous carbons of SDCCB are feasibly a good substitute for other commercially available activated carbons produced from natural resources. Also, the antimicrobial studies reveal that SDCCB exhibits significant cytotoxicity and enzymatic inhibitory activities and it is a potential candidate for further investigation.

CONSENT

It is not applicable.

ETHICAL APPROVAL

It is not applicable.

COMPETING INTERESTS

Authors have declared that no competing interests exist.

REFERENCES

1. Han R, Zou W, Li H, Li Y, Shi J. Copper(II) and lead(II) removal from aqueous solution

in fixed-bed columns by manganese oxide coated zeolite. Journal of Hazardous Materials. 2006;137(2):934-942.

2. Gong JL, Wang XY, Zeng GM, Chen L, Deng JH, Zhang XR, Niu QY. Copper(II) removal by pectin–iron oxide magnetic nano composite adsorbent. Chemical Engineering Journal. 2012;185:100-107.
3. Panday KK, Prasad G, Singh VN. Copper(II) removal from aqueous solutions by fly ash. Water Research. 1985;19(7): 869-873.
4. Kyzas GZ, Deliyanni EA, Matis KA. Activated carbons produced by pyrolysis of waste potato peels: Cobalt ions removal by adsorption. Colloids and Surfaces A: Physicochemical and Engineering Aspects. 2016;490:74-83.
5. Mohan D, Chander S. Single component and multi-component adsorption of metal ions by activated carbons. Colloids and Surfaces A: Physicochemical and Engineering Aspects. 2001;177(2-3):183-196.
6. Alhaji NMI, Tajun Meera Begum KM. Optimization and kinetic study for the removal of chromium(VI) ions by acid treated sawdust chitosan composite beads. International Research Journal of Pure & Applied Chemistry. 2015;5(2):160-176.
7. Vinodhini V, Das N. Relevant approach to assess the performance of sawdust as adsorbent of chromium(VI) ions from aqueous solutions. Int. J. Environ. Sci. Tech. Winter. 2010;7(1):85-92.
8. Begum KMTM, Alhaji NMI. Spectro-photometric determination of the efficiency of lignocellulosic sludge-based adsorbents in the removal of Cr(VI) and Ni(II) ions from aqueous solution. Chemical Science. 2016;5(3):523-540.
9. Han R, Zou L, Zhao X, Xu Y, Xu F, Li Y, Wang Y. Characterization and properties of iron oxide-coated zeolite as adsorbent for removal of copper(II) from solution in fixed bed column. Chemical Engineering Journal. 2009;149(1-3):123-131.
10. Demiral H, Güngör C. Adsorption of copper(II) from aqueous solutions on activated carbon prepared from grape bagasse. Journal of Cleaner Production. 2016;124:103-113.
11. Hallett MT, Lagergren J. New algorithms for the duplication-loss model. In Proceedings of the Fourth Annual International Conference on Computational Molecular Biology. 2000;138-146.
12. Tien C, Ramarao BV. On the significance and utility of the Lagergren model and the pseudo second-order model of batch adsorption. Separation Science and Technology. 2017;52(6):975-986.
13. Faur-Brasquet C, Kadirvelu K, Le Cloirec P. Removal of metal ions from aqueous solution by adsorption onto activated carbon cloths: Adsorption competition with organic matter. Carbon. 2002;40(13):2387-2392.
14. Moosa S, Nemati M, Harrison ST. A kinetic study on anaerobic reduction of sulphate, part II: Incorporation of temperature effects in the kinetic model. Chemical Engineering Science. 2005;60(13):3517-3524.
15. Faur-Brasquet C, Kadirvelu K, Le Cloirec P. Removal of metal ions from aqueous solution by adsorption onto activated carbon cloths: Adsorption competition with organic matter. Carbon. 2002;40(13):2387-2392.
16. Cestari AE, Vieira EFS, Mota JA. The removal of an anionic red dye from aqueous solutions using chitosan beads – The role of experimental factors on adsorption using a full factorial design. J. Hazard. Mater. 2008;160:337-343.
17. Ho YS, McKay G. Sorption of copper(II) from aqueous solution by peat. Water, Air, and Soil Pollution. 2004;158(1):77-97.
18. Hawkins RB. A microdosimetric-kinetic model for the effect of non-Poisson distribution of lethal lesions on the variation of RBE with LET. Radiation Research. 2003;160(1):61-69.
19. Fu W, Mathews AP. Lactic acid production from lactose by *Lactobacillus plantarum*: Kinetic model and effects of pH, substrate, and oxygen. Biochemical Engineering Journal. 1999;3(3):163-170.
20. Goujard V, Tatibouët JM, Batiot-Dupeyrat C. Carbon dioxide reforming of methane using a dielectric barrier discharge reactor: Effect of helium dilution and kinetic model. Plasma Chemistry and Plasma Processing. 2011;31(2):315-325.
21. Alhaji NMI, Uduman Mohideen AM, Sofia Lawrence Mary S. Mechanism of oxidation of (p-substituted phenylthio) acetic acids with N-chlorosaccharin. e-Journal of Chemistry. 2011;8(1):159-166.
22. Smith GG, Sivakua T. Mechanism of the racemization of amino acids. Kinetics of racemization of arylglycines. The Journal

of Organic Chemistry. 1983;48(5):627-634.

23. Fiebich BL, Biber K, Lieb K, Van Calker D, Berger M, Bauer J, Gebicke-Haerter PJ. Cyclooxygenase-2 expression in rat microglia is induced by adenosine A2a-receptors. Glia. 1996;18(2):152-180.
24. Ayeshamariam A, Saravanakkumar D, Kashif M, Sivaranjani S, Ravikumar B. Analysis on the effect of ZnO on carbon nanotube by spray pyrolysis method. Mechanics of Advanced Materials and Modern Processes. 2016;2(1):3.
25. Mohammadi A, Rafiee S, Emam-Djomeh Z, Keyhani A. Kinetic models for colour changes in kiwifruit slices during hot air drying. World Journal of Agricultural Sciences. 2008;4(3):376-383.
26. Dursun AY, Kalayci CS. Equilibrium, kinetic and thermodynamic studies on the adsorption of phenol onto chitin. Journal of Hazardous Materials. 2005;123(1-3):151-157.
27. Kayalvizhi K, Alhaji NMI. Removal of copper using activated carbon adsorbent and its antibacterial antifungal activity. European Journal of Medicinal Plants. 2020;24-33.
28. Raza K, Kumar D, Kiran C, Kumar M, Guru SK, Kumar P, Arora S, Sharma G, Bhushan S, Katare OP. Conjugation of docetaxel with multiwalled carbon nanotubes and codelivery with piperine: implications on pharmacokinetic profile and anticancer activity. Molecular Pharmaceutics. 2016;13(7):2423-2432.

Peer-review history:
The peer review history for this paper can be accessed here:
http://www.sdiarticle4.com/review-history/55481